ACS APPLIED MATERIALS & INTERFACES

Letter

www.acsami.org

Bendable Photodetector on Fibers Wrapped with Flexible Ultrathin Single Crystalline Silicon Nanomembranes

Enming Song, Qinglei Guo, Gaoshan Huang, Bo Jia, and Yongfeng Mei*

Department of Materials Science, Fudan University, 220 Handan Road, Shanghai 200433, China

Supporting Information

ABSTRACT: Silicon (Si) nanomembranes (NMs) enable conformal covering on complicated surfaces for novel applications. We adopt classical fibers as flexible/curved substrates and wrap them with freestanding ultrathin Si-NMs with a thickness of ~20 nm. Intrinsic defects in single-crystalline Si-NMs provide a flow path for hydrofluoric acid (HF) to release the NM with a consecutive area of ~0.25 cm^2. Such Si-NMs with ultralow flexural rigidities are transferred onto a single-mode fiber (SMF) and functionalized into bendable photodetectors, which detects the leaked light when the fiber is bent. Our demonstration exemplifies optoelectronic applications in flexible photodetector for Si-NMs in a three-dimensional (3D) geometry.

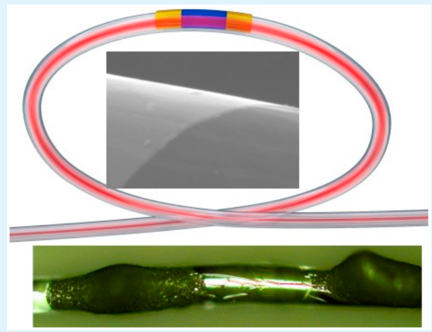

KEYWORDS: *ultrathin silicon nanomembrane, transfer technology, optical fiber, photodetector, Schottky barrier*

Because of their high-performance optical and electrical properties, flexible inorganic nanomembranes[1−3] have attracted considerable attention recently in extensive applications of, for example, hemispherical electronic eye camera,[4] transferrable micro lasing devices,[5] stretchable single photon source,[6] strain-relaxed strained-silicon,[7] and implantable cardiac electrophysiological mapping.[8] Two-dimensional (2D) geometry of nanomembrane presents the capability of conformal wrapping on complex and curvilinear surfaces even like human skin by a mechanically "invisible" contact.[9] Recently, substantial efforts have been explored to assemble flexible devices by utilizing single-crystalline silicon nanomembranes (Si-NMs)[10,11] as building blocks, which are drawing increasing attentions as the promising candidates for flexible photodetectors because of their superior mechanical, electrical and optical properties.[12] In regard to applications of various flexible photodetectors,[13−17] light leakage detecting is frequently of concern, which is crucial to many fields, especially to optical fibers. On the other hand, classical optical fibers, as an essential component for communications, medicine, and sensing[18] exhibit excellent bending capability with low light leakages. However, such leakage could influence the signal communication if the bending is big enough, which attracted research to reduce or quantify the leakages.[19,20] In this respect, photodetectors with superior mechanical flexibility, high resolution, and ultrasensitivity are urgent demanded to locally sense the light leakages on fibers in a conformal manner. Hence, it is expected that flexible single crystalline silicon nanomembranes can well-attach on the curved surface of fibers and present a bending photodetectors for light leakage when the fiber is bent.

Here, we demonstrate a convenient strategy to construct flexible photodetectors wrapped on an optical single-mode fiber (SMF) by utilizing ultrathin Si-NMs with thickness of about 20 nm released from silicon-on-insulator (SOI). The obtained consecutive Si-NM with a large area (~5 × 5 mm^2) is wrapped on a bendable SMF as semiconductor materials for metal—semiconductor-metal (MSM) photodetector, which is constructed by depositing silver paste as electrodes. The Schottky contact of Si-NMs with electrodes for MSM photodetectors can be tuned by illumination under thermionic emission (TE) mechanism. Such device demonstrates a scheme to locally sense light leakage on optical fibers and presents sensitive light detection even with a small bending of fibers with the curvature down to 0.1 cm^{-1}, which agrees with the bending loss calculations.

The release of ultrathin SiNMs starts with a (001) SOI wafer (Figure 1a) with boron doped top silicon layer. Here we used four point probe (Jandel Four Point Probe, RM3000 Test Unit) to measure a resistivity of Si-NM as a value of 11.51 Ω cm, corresponding to a boron doping level of ~1 × 10^{16} cm^{-3} according to a previous report.[21] To demonstrate that the single-crystalline Si-NM is ultrathin, we manifest a characterization on SOI cross section by transmission electron microscope (TEM, Philips CM200FEG) image, which displays the Si-NM thickness is ~16.1 nm (Figure 1a). An upper oxide layer (~3 nm) forms on Si-NM and then a protecting platinum layer (~3 nm thick) was deposited on top. This Si-NM has excellent single-crystal structure, as shown in a high resolution transmission electron microscope (HR-TEM, Philips CM200FEG) image in Figure 1b. The inset is corresponding diffraction spectroscopy.

Received: February 13, 2017
Accepted: March 29, 2017
Published: March 29, 2017

DOI: 10.1021/acsami.7b02123
ACS Appl. Mater. Interfaces 2017, 9, 12171−12175

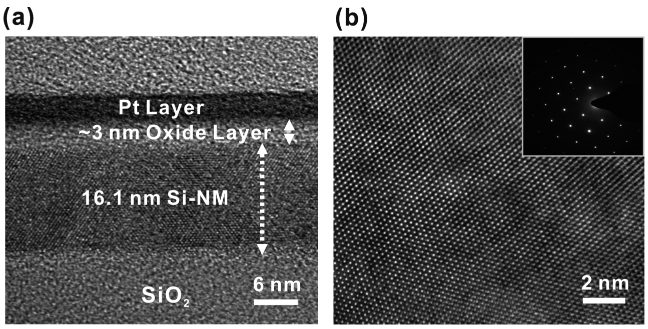

Figure 1. (a) Cross-sectional TEM image of a typical ultrathin Si-NM with a thickness of ∼16.1 nm. (b) HR-TEM image of a single-crystalline Si-NM and corresponding inset of diffraction spectroscopy.

Despite superior crystalline structure, defects existing in single-crystalline semiconductors could influence the corresponding crystalline structures and optoelectrical properties.[22,23] As revealed in Figure S1a−c, there are many intrinsic defects (white spots) distributed throughout large Si-NMs, which provide tiny holes for the flowing of HF vapor. Such defect or dislocation assistant etching was observed in previous work and help the release and self-assembly of GaN NMs.[24,25] Facilitated by these defect-consisted passages, the silicon oxide layer in SOI can be thoroughly removed under sufficient etching time (about 30 min). As a result, a large area of Si-NM (∼0.25 cm^2) with high flexibility was released and transferred onto a SMF. Detailed process is schematically illustrated in Figure S2.

Figure 2a is a schematic diagram of a Si-NM photodetector device on a bendable 20 cm long fiber which guides light. When SMF is bent, some portion of light in fiber is likely to leak from core to the outer surface and then absorbed by the Si-NM device. Figure 2b shows the constructed Si-NM based photodetector on a bendable and flexible SMF (inset). The flexible Si-NM is functionalized into a double-electrode photodetector contacted with silver paste. The channel length of the detector is ∼100 μm. Such a device can hold external mechanical stress without any obvious cracks formed in the Si-NM, as proved by the optical microscopy results in Figure 2b and the inset. To verify the strain state, we carefully carried out micro-Raman measurements on Si-NMs on fibers. Mechanical strain/stress in Si-NMs might influence their frequency of Raman vibration modes,[26] thus makes the corresponding devices unstable and yields degeneracy. Also, micro-Raman spectroscopy was proved to be an effective method to quantitatively evaluate the residual strain/stress distributed in Si-NMs by Raman peak shifts.[27] Specifically, we started with a 20 cm straight long fiber with a Si-NM wrapped on it and then bended into various curvature angles (straight line and loop corresponding to 0 and 360°, respectively). Raman spectra on same position with various curvature angles (30° as a step, from 0−360°) are displayed in Figure S3, where there are almost no shifts. Noting that Si-NM length is ∼1 × 10^3 fold smaller than fiber, bending of fiber into various curvatures has much less influence on Si-NM. At 360°, the curvature of Si-NM device is inconspicuous in Figure 2b, which might lead to the residual stress in Si-NM being considerably small.

On the basis of the flexible Si-NM-on-fiber structure, Figure 2c presents the electrical characteristic of Si-NM-based photodetectors on SMF without bending (no curvature) when laser light is transporting (illuminated, red dots) or not (dark, black squares). It is revealed that such an Si-NM-based device is under Schottky contacts in both ends under both illuminated and dark cases. To further prove that bending SMFs will not generate obvious mechanical strain in Si-NMs, we characterized the current cross the Si-NM channel in dark and show it in Figure S4a with various bending states, whose curvatures are 0, 0.2, and 0.5 cm^{-1}. Electrical performances of Si-NM-based photodetector wrapping on SMF with different curvatures in dark remain almost same under varying bias (V_B), which elucidates that the mechanical strain induced by bending can be negligible. Hence, the electrical current changes in Si-NM-based photodetector wrapping around the SMF under illumination can be attributed to light-induced photocurrents. In our experiments, the illumination method is realized by simply coupling a laser light into one end of SMF. It is worth noting that the photocurrent (red dots in Figure 2c) of ultrathin Si-NM-based photodetector is dramatically enhanced for almost three times when the coupled light passes though the SMF compared with the dark current (black squares). Furthermore, the transient response properties of the detector are measured by repeatedly switch on and off laser light (no

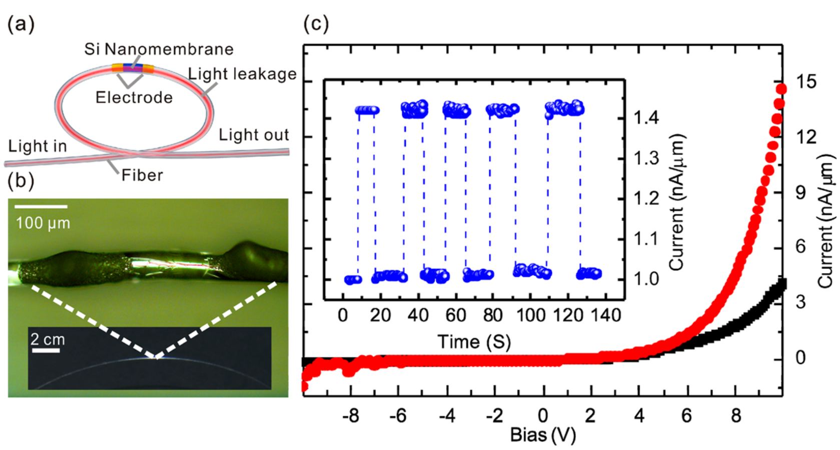

Figure 2. (a) Schematic diagram of a Si-NM-based photodetector on a bendable optical fiber. (b) OM image shows a bended Si-NM-wrapped SMF device with two Ag paste electrodes and the inset is an optical image of a bended fiber with our constructed device. (c) Electrical characteristic of Si-NM-based SMF device under illumination (Illuminated, red dots) and in dark (Dark, black squares) without bending. Inset, dynamic photocurrent as a function of time at fixed bias V_B = 6 V when the light source is on and off.

DOI: 10.1021/acsami.7b02123
ACS Appl. Mater. Interfaces 2017, 9, 12171−12175

bending) with fixed V_B of 6 V, as shown in the inset of Figure 2c. The photoelectric response exhibits high photocurrent, good stability with constant illuminated and dark currents and fast response time with steep rising and falling edges. The related mechanism of band profile in Si-NMs is discussed in Figure S4b.

According to the phenomenon that Si-NM-based photodetector wrapping on the SMF is ultrasensitive to light illumination, we exploit the device to detect the light leakages of the SMF during different bending states. Figure 3a shows the photoelectric response property of the SiNM-based photodetector under various mechanical bending states when changing the SMF curvature from 0 to 0.5 cm^{-1}. The electrical conductivity of Si-NMs exhibits distinct increase, as the bending curvature of the SMF increases. With increasing curvature, the original situation of attenuated total reflectance (ATR) is slightly destroyed. More light transport inside the SMF is able to leak out from the core toward the Si-NM/SMF interface, inducing more light absorption in the Si-NM surface. The relationships between photocurrent and curvatures respecting to dark (I_{Dark}) and illumination (I_{Light}) situations are summarized in Figure 3b, which implies that the photocurrent is increased exponentially to the curvature (the fitting curve: I_{Light} = 1.19exp(7.7curvature) + 14.35 in Figure 3b) at a 10 V bias, whereas I_{Dark} remains almost the same when the SMF is curved. Hence, the bending loss of light has a great influence on the electrical performances of our Si-NM-wrapped SMF device. Recent work shows that SiNMs can absorb photons effectively when light penetrates.[10] The relation between light power P in the membrane and penetration depth x can be written as eq 1

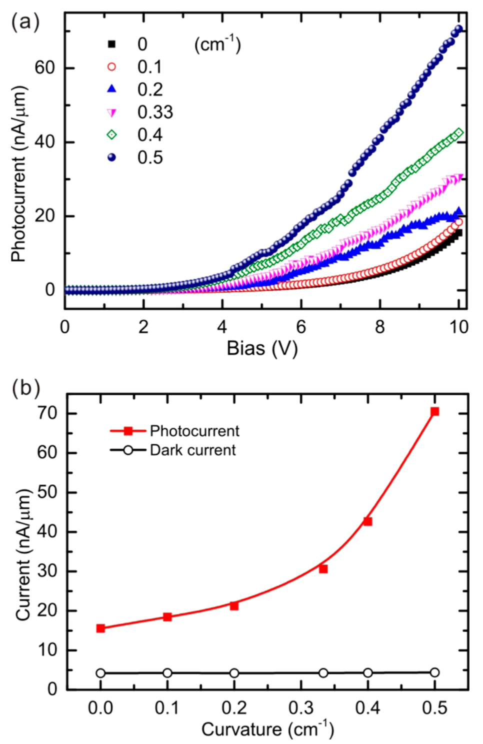

Figure 3. (a) Current versus bias (I–V) curves of Si-NMs under illumination with various bending curvatures (0, 0.1, 0.2, 0.33, 0.4, and 0.5 cm^{-1}). (b) Photocurrent (I_{Light}) and dark current (I_{Dark}) as a function of SMF bending curvatures under a fixed bias (V_B = 10 V). The respective curvatures are 0, 0.1, 0.2, 0.33, 0.4, and 0.5 cm^{-1}.

$$P = P_0 \exp(\alpha x) \quad (1)$$

,where P_0 is the power at the surface of the membranes and α is the corresponding absorption coefficient. In fact, the "absorbance" is a measure of the amount of light absorbed by the sample under specified conditions. For a Si sample with thickness of d, the average light absorbance per thickness is defined as $\left(\frac{P_0 - P_0\exp(-\alpha d)}{d}\right)$. In the case of Si with smaller d, for example, Si-NMs, the average light absorbance becomes much larger than that in bulk Si. The special characteristic of ultrathin thickness makes Si-NMs have great potential applications as sensitive photodetectors.

Numerical simulation[28] demonstrates the bend loss of light in single-mode and multimode fibers with step-index, which is expected to be characterized by our bendable photodetectors. The inset of Figure 4 illustrates a schematic of a bended SiNM-SMF device when light is guided through the fiber. P_{in} is the initial power and P_{out} is the emitted light power after the bend loss ΔP and R is the bending radius. P_{in} and P_{out} were measured by a SCIENTECH 312 power and energy meter at the start and end of a loop. P_{in} is 8 mW. Figure 4 shows the bending loss dB/cm and I_{Light}/I_{Dark} values (data from Figure 3b) varying with the curvatures of SMF, where I_{Light} is photocurrent and I_{Dark} is dark current. The bending loss caused by curvature, as shown by the blue spheres, is obtained by calculating the amount of power outflow per unit length of waveguide and substituting into the loss formula, written as eq 2

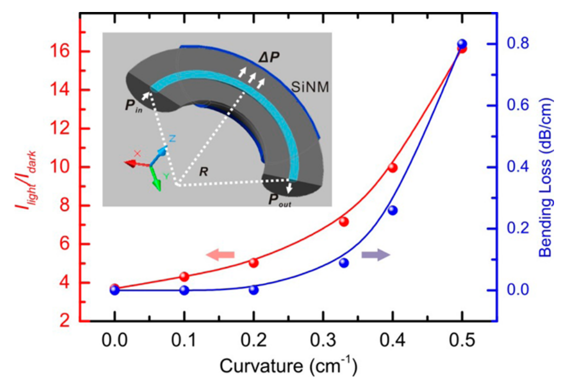

Figure 4. (Left) Ratio of photocurrent (I_{light}) and dark current (I_{dark}) as a function of fiber curvatures and (Right) calculated bending loss (dB/cm). The electrical current is measured at a fixed bias (V_B = 10 V). Inset, sketch of a bended fiber with light in and out through a fiber. When fiber is bended at X-Y planar, the light leakage increases from core to the cladding layer and finally is absorbed by wrapped Si-NMs. P_{in} is the inlet power and P_{out} is the outlet light power with a bend loss ΔP. R is the bend radius.

$$\alpha = 10\log_{10}(P_{in}/P_{out}) \quad (2)$$

where α is the power loss coefficient with the unit as dB/cm. Theoretical reference has given the loss formula that indicated such loss coefficient depends on the radius R of fiber curvature when placed in a specified condition.[28,29] The values of dB/cm in Figure 4 under different bending curvatures, as shown blue line, are theoretical calculation as $\alpha = AR^{-1/2}\exp(-CR)$ where A and C are fixed constants, and R is bending radius depending on previous work,[29] with a wavelength of 633 nm. The fitting values for A and C here are 60.61 and 1.99, respectively. Light propagating along the SMF has nearly no bending loss ($\alpha < 0.1$ dB/cm, $P_{out}/P_{in} > 99\%$) until a critical bend radius (∼0.33 cm^{-1}) arrives. Continued bending, the bend loss of dB/cm increases with the curvature in an exponential manner. When the curvature exceeds 2 cm^{-1}, almost all the light will leak out from the SMF with the value of power loss $P_{out}/P_{in} < 0.01\%$. Meanwhile the ratio of I_{Light}/I_{Dark} increases exponentially with the curvatures of the SMF (red spheres in Figure 4), which means the light leakage is absorbed by the surrounding Si-NMs, leading to sensitive photodetection.

In summary, we have demonstrated a Si-NM-wrapped fiber can be constructed as a flexible and bending photodetector for sensing the bending loss of light. HF vapor etching is employed to release ultrathin Si-NMs with the thickness of about 20 nm with a large area of consecutive Si-NM (∼0.25 cm^2). The released bendable Si-NMs have ultralow flexural rigidity and high average light absorbance per thickness. The photoelectric response property of Si-NMs is addressed to detect the light leakage in a bendable optical fiber. Such Si-NM-based optoelectrical device can well-detect light crossing the fiber and sensing the bending curvatures down to 0.1 cm^{-1}. Our study on flexible Si-NM-SMF photodetectors might hint at new applications in optoelectronics and photonics for flexible silicon nanomembranes.

■ ASSOCIATED CONTENT

Supporting Information

The Supporting Information is available free of charge on the ACS Publications website at DOI: 10.1021/acsami.7b02123.

Microstructure characterization of Si-NM, release and transfer of silicon nanomembranes, Raman spectroscopy measurement, optoelectrical measurements, and related experimental details are given (PDF)

■ AUTHOR INFORMATION

Corresponding Author

*E-mail: yfm@fudan.edu.cn.

ORCID

Enming Song: 0000-0002-2658-904X

Yongfeng Mei: 0000-0002-3314-6108

Funding

Natural Science Foundation of China Specialized Research Fund for the Doctoral Program of Higher Education Science and Technology Commission of Shanghai Municipality

Notes

The authors declare no competing financial interest.

■ ACKNOWLEDGMENTS

This work is supported by the Natural Science Foundation of China (51322201 and U1632115), Science and Technology Commission of Shanghai Municipality (14JC1400200), the National Key Technologies R&D Program of China (2015ZX02102-003) and the Changjiang Young Scholars Programme of China. Part of the experimental work has been carried out in Fudan Nanofabrication Laboratory.

■ REFERENCES

(1) Rogers, J. A.; Lagally, M. G.; Nuzzo, R. G. Synthesis, Assembly, and Applications of Semiconductor Nanomembranes. *Nature* **2011**, *477*, 45−53.

(2) Cavallo, F.; Lagally, M. G. Semiconductors Turn Soft: Inorganic Nanomembranes. *Soft Matter* **2010**, *6*, 439−455.

(3) Huang, G. S.; Mei, Y. F. ChemInform Abstract: Thinning and Shaping Solid Films into Functional and Integrative Nanomembranes. *Adv. Mater.* **2012**, *24*, 2517−2546.

(4) Ko, H. C.; Stoykovich, M. P.; Song, J.; Malyarchuk, V.; Choi, W. M.; Yu, C.-J.; Geddes, J. B., III; Xiao, J.; Wang, S.; Huang, Y.; Rogers, J. A. A Hemispherical Electronic Eye Camera Based on Compressible Silicon Optoelectronics. *Nature* **2008**, *454*, 748−753.

(5) Yang, H. J.; Zhao, D. Y.; Chuwongin, S.; Seo, J.-H.; Yang, W. Q.; Shuai, Y. C.; Berggren, J.; Hammar, M.; Ma, Z. Q.; Zhou, W. D. Transfer-Printed Stacked Nanomembrane Lasers on Silicon. *Nat. Photonics* **2012**, *6*, 615−620.

(6) Huo, Y. H.; Witek, B. J.; Kumar, S.; Cardenas, J. R.; Zhang, J. X.; Akopian, N.; Singh, R.; Zallo, E.; Grifone, R.; Kriegner, D.; Trotta, R.; Ding, F.; Stangl, J.; Zwiller, V.; Bester, G.; Rastelli, A.; Schmidt, O. G. A Light-Hole Exciton in a Quantum Dot. *Nat. Phys.* **2014**, *10*, 46−51.

(7) Roberts, M. M.; Klein, L. J.; Savage, D. E.; Slinker, K. A.; Friesen, M.; Celler, G.; Eriksson, M. A.; Lagally, M. G. Elastically Relaxed Free-Standing Strained-Silicon Nanomembranes. *Nat. Mater.* **2006**, *5*, 388−393.

(8) Kim, D.-H.; Lu, N.; Ghaffari, R.; Kim, Y.-S.; Lee, S. P.; Xu, L.; Wu, J.; Kim, R.-H.; Song, J.; Liu, Z.; Viventi, J.; de Graff, B.; Elolampi, B.; Mansour, M.; Slepian, M. J.; Hwang, S.; Moss, J. D.; Won, S.-M.; Huang, Y.; Litt, B.; Rogers, J. A. Materials for Multifunctional Balloon Catheters with Capabilities in Cardiac Electrophysiological Mapping and Ablation Therapy. *Nat. Mater.* **2011**, *10*, 316−323.

(9) Rogers, J. A.; Someya, T.; Huang, Y. G. Materials and Mechanics for Stretchable Electronics. *Science* **2010**, *327*, 1603−1607.

(10) Song, E. M.; Si, W. P.; Cao, R. G.; Feng, P.; Mönch, I.; Huang, G. S.; Di, Z. F.; Schmidt, O. G.; Mei, Y. F. Schottky Contact on Ultra-Thin Silicon Nanomembranes Under Light Illumination. *Nanotechnology* **2014**, *25*, 485201.

(11) Feng, P.; Mönch, I.; Harazim, S.; Huang, G. S.; Mei, Y. F.; Schmidt, O. G. Giant Persistent Photoconductivity in Rough Silicon Nanomembranes. *Nano Lett.* **2009**, *9*, 3453−3459.

(12) Lu, C. F.; Li, M.; Xiao, J. L.; Jung, I.; Wu, J.; Huang, Y.; Hwang, K.-C.; Rogers, J. A. Mechanics of Tunable Hemispherical Electronic Eye Camera Systems That Combine Rigid Device Elements With Soft Elastomers. *J. Appl. Mech.* **2013**, *80*, 061022.

(13) Kim, J.; Joo, S. S.; Lee, K. W.; Kim, J. H.; Shin, D. H.; Kim, S.; Choi, S.-H. Near-Ultraviolet-Sensitive Graphene/Porous Silicon Photodetectors. *ACS Appl. Mater. Interfaces* **2014**, *6*, 20880.

(14) Chen, T.-G.; Huang, B.-Y.; Liu, H. W.; Huang, Y.-Y.; Pan, H.-T.; Meng, H.-F.; Yu, P. Flexible Silver Nanowire Meshes for High-Efficiency Microtextured Organic-Silicon Hybrid Photovoltaics. *ACS Appl. Mater. Interfaces* **2012**, *4*, 6857.

(15) Liu, X.; Ji, X.; Liu, M.; Liu, N.; Tao, Z.; Dai, Q.; Wei, L.; Li, C.; Zhang, X.; Wang, B. High-Performance Ge Quantum Dot Decorated Graphene/Zinc-Oxide Heterostructure Infrared Photodetector. *ACS Appl. Mater. Interfaces* **2015**, *7*, 2452.

(16) Bao, C.; Zhu, W.; Yang, J.; Li, F.; Gu, S.; Wang, Y.; Yu, T.; Zhu, J.; Zhou, Y.; Zou, Z. Highly Flexible Self-Powered Organolead Trihalide Perovskite Photodetectors with Gold Nanowire Networks as Transparent Electrodes. *ACS Appl. Mater. Interfaces* **2016**, *8*, 23868.

(17) Li, L.; Lou, Z.; Shen, G. Hierarchical CdS Nanowires Based Rigid and Flexible Photodetectors with Ultrahigh Sensitivity. *ACS Appl. Mater. Interfaces* **2015**, *7*, 23507.

(18) Barrias, A.; Casas, J. R.; Villalba, S. A Review of Distributed Optical Fiber Sensors for Civil Engineering Applications. *Sensors* **2016**, *16*, 748.

(19) Li, M. J.; Tandon, P.; Bookbinder, D. C.; Bickham, S. R.; McDermott, M. A.; Desorcie, R. B.; Nolan, D. A.; Johnson, J. J.; Lewis, K. A.; Englebert, J. J. Ultra-Low Bending Loss Single-Mode Fiber for FTTH. *J. Lightwave Technol.* **2009**, *27*, 376−382.

(20) Schermer, R. T.; Cole, J. H. Improved Bend Loss Formula Verified for Optical Fiber by Simulation and Experiment. *IEEE J. Quantum Electron.* **2007**, *43*, 899−909.

DOI: 10.1021/acsami.7b02123
ACS Appl. Mater. Interfaces 2017, 9, 12171−12175

(21) Arora, N. D.; Hauser, J. R.; Roulston, D. J. Electron and Hole Motilities in Silicon as a Function of Concentration and Temperature. *IEEE Trans. Electron Devices* **1982**, *29*, 292−295.
(22) Scott, S. A.; Lagally, M. G. Elastically Strain-Sharing Nanomembranes: Flexible and Transferable Strained Silicon and Silicon−Germanium Alloys. *J. Phys. D: Appl. Phys.* **2007**, *40*, 75−92.
(23) Léonard, F.; Talin, A. A. Electrical Contacts to One- and Two-Dimensional Nanomaterials. *Nat. Nanotechnol.* **2011**, *6*, 773−783.
(24) Mei, Y. F.; Thurmer, D. J.; Deneke, C.; Kiravittaya, S.; Chen, Y.-F.; Dadgar, A.; Bertram, F.; Bastek, B.; Krost, A.; Christen, J.; Reindl, T.; Stoffel, M.; Coric, E.; Schmidt, O. G. Fabrication, Self-Assembly, and Properties of Ultrathin AlN/GaN Porous Crystalline Nanomembranes: Tubes, Spirals, and Curved Sheets. *ACS Nano* **2009**, *3*, 1663−1668.
(25) Elafandy, R. T.; Majid, M. A.; Ng, T. K.; Zhao, L.; Cha, D.; Ooi, B. S. Nanomembranes: Exfoliation of Threading Dislocation-Free, Single-Crystalline, Ultrathin Gallium Nitride Nanomembranes. *Adv. Funct. Mater.* **2014**, *24*, 2305−2311.
(26) Yamaguchi, M.; Ueno, S.; Miura, I.; Erikawa, W. Experimental Mechanical Stress Characterization of Micro-Electro-Mechanical-Systems Device Using Confocal Laser Scanning Microscope Combined with Raman Spectrometer System. *Jpn. J. Appl. Phys.* **2007**, *46*, 6860−6862.
(27) Guo, Q. L.; Zhang, M.; Xue, Z. Y.; Ye, L.; Wang, G.; Huang, G. S.; Mei, Y. F.; Wang, X.; Di, Z. F. Three Dimensional Strain Distribution of Wrinkled Silicon Nanomembranes Fabricated by Rolling-Transfer Technique. *Appl. Phys. Lett.* **2013**, *103*, 264102−264105.
(28) Marcuse, D. Curvature Loss Formula for Optical Fibers. *J. Opt. Soc. Am.* **1976**, *66*, 216−220.
(29) Watekar, P. R.; Ju, S.; Han, W.-T. Bend Insensitive Optical Fiber with Ultralow Bending Loss in the Visible Wavelength Band. *Opt. Lett.* **2009**, *34*, 3830−3832.

DOI: 10.1021/acsami.7b02123
ACS Appl. Mater. Interfaces 2017, 9, 12171−12175